THE JOURNAL OF NAVIGATION (2019), **72**, 1035–1052.
doi:10.1017/S0373463318001078

Ship Heading Control with Speed Keeping via a Nonlinear Disturbance Observer

Zhiquan Liu, Xiaoyang Lu and Diju Gao

(*Key Laboratory of Marine Technology and Control Engineering Ministry of Communications, Shanghai Maritime University, Shanghai 201306 China*)
(E-mail: liuzhiquan215@sina.com)

The control problem for a ship steering system with speed loss is discussed in this paper. Two methods are proposed to deal with the unknown bounded disturbance for a sliding mode controller applied to a nonlinear surface vessel heading control system. The system uncertainties caused by speed changes are taken as internal disturbances, while the wave moments are considered as external disturbances. A feedback linearization method is adopted to simplify the nonlinear system. An adaptive method and a Nonlinear Disturbance Observer (NDO) are proposed for course keeping manoeuvres and speed keeping in vessel steering and provide robust performance for time varying wave disturbance and actuator dynamics. Furthermore, the overall stability conditions of the proposed controllers are analysed by Lyapunov's direct method. Finally, simulation results using the characteristics of a naval vessel illustrate the effectiveness of the presented control algorithms.

KEYWORDS

1. Course keeping. 2. Speed loss. 3. Sliding mode control. 4. NDO.

Submitted: 19 November 2017. Accepted: 10 December 2018. First published online: 22 January 2019.

1. INTRODUCTION. When a surface vessel is sailing in a seaway, waves which cause external forces and moments play an important role in its manoeuvring characteristics. These external forces and moments usually induce six degree of freedom (DOF) motions that affect the capacity of surface vessels to achieve their missions and may cause cargo damage. Therefore, some devices need to be applied to maintain vessel stability and orientation. A ship's autopilot system is used to ensure a ship navigates on the desired course by manipulating the rudder angle (Fang and Luo, 2005). Major contributions to the development of practical steering systems were made by the Sperry Gyroscope Company. The first automatic ship steering mechanism was constructed in 1911, and a detailed theoretical analysis of a Proportional Integral Derivative (PID) controller for ship steering was presented by Nicholas Minorsky in 1922, where the yaw angle of the vessel was measured by a gyrocompass (Fossen, 2011; Roberts, 2008).

Ocean going vessel steering autopilots are designed to implement course keeping and course changing manoeuvres in the open sea (Burns, 1995; Tzeng, 1999). The classical

PID controller with fixed gain is a conventional steering controller and it can give a good performance for particular operating conditions, such as track keeping control, rudder/fin roll stabilisation and heading control with an identified model (Fang and Luo, 2006; Fang et al., 2012; Banazadeth and Ghorbani, 2013). Some other linear controllers have also been applied to autopilot control systems, such as the internal model controller and the model predictive controller (Saari and Djemai, 2012; Liu et al., 2015). Li and Sun (2012) addressed a disturbance compensating model predictive heading controller to satisfy the state constraints.

One of the major issues in modern ship control systems is to guarantee robust stability and performance under uncertain environment disturbances and linear controllers cannot always achieve this. Several types of nonlinear controllers have been proposed to overcome the nonlinear steering problem in recent literature, such as feedback linearization, Sliding Mode Control (SMC) and an adaptive method. The typical state feedback linearization and input output linearization methods have been adopted in autopilot control systems (Moreira et al., 2007; Borkowski, 2014; Perera and Soares, 2013). Zhang and Zhang (2016) introduced a sine function nonlinear feedback controller for surface ship heading control. The nonlinear state or parameters in ship steering dynamics are often linearized around specific points in these controllers and always deal with known bounded disturbances. Sliding mode control is based on the Lyapunov stability theorem and a large number of papers are available on ship control. For surface vessels, Zhang et al. (2000) discussed the path following control problem in restricted waters. Alfaro-Cid et al. (2005) developed two decoupled sliding mode controllers for ship navigation and propulsion. Fang and Luo (2007) compared two sliding mode controllers for roll reduction and a track keeping control system. Harl and Balakrishnan (2012) considered a second order sliding mode control strategy for path following. Perera and Soares (2012) proposed a pre-filtered sliding mode control law to solve the nonlinear steering dynamic problem (that is, parameter uncertainties and un-modelled dynamics).

Ship dynamics can be influenced significantly due to sailing conditions and unpredictable environmental disturbances, which may affect the efficiency of crews, the accuracy of electrical mechanisms and reduce the abilities of vessels to perform their missions. Therefore, a nonlinear controller that overcomes unknown bounded external disturbances and guarantees robustness is needed. An adaptive method can be a good method to deal with these uncertainties. In the area of surface vessels, a robust adaptive controller based on Lyapunov's direct method was proposed to estimate the values of ship unknown parameters and cope with the bounded time varying terms of environmental disturbances (Do and Pan, 2006). An adaptive Neural Network (NN) method was developed to counter the unknown information of the hydrodynamic structure (Zhang et al., 2015; Shojaei, 2015). The adaptive technique was also combined with Dynamic Surface Control (DSC), fuzzy and backstepping methods (Peng et al., 2013; Li et al., 2013; Lin et al., 2014). In the area of underwater vehicle tracking control, Do (2015) introduced a robust adaptive controller for an Omnidirectional Intelligent Navigator (ODIN) tracking under stochastic environmental loads and Liu et al. (2016) considered an adaptive fuzzy NN controller for an Unmanned Underwater Vehicle (UUV) that was subjected to unknown disturbances and dynamic uncertainties. Another method to reject the unknown bounded disturbance is called a disturbance observer. The observer method is always combined with a nonlinear controller for a ship motion control system, such as the backstepping method and the sliding mode controller (Liu et al., 2011; Xu et al., 2016). Lei and Guo (2015) proposed an extended observer

https://doi.org/10.1017/S0373463318001078 Published online by Cambridge University Press

to estimate the total disturbances of the ship steering system. A disturbance observer was employed with the dynamic surface control technique for a ship dynamic positioning system by Du et al. (2016). Still aiming at the track following and course keeping problems, to overcome the uncertain environmental disturbances under sensorless conditions, Qin et al. (2016) developed a sliding mode controller with a high gain observer for an underactuated ship. These studies are limited to surface vessel course keeping control under the assumption that the forward speed is constant.

Ships that proceed at certain speeds in open sea usually encounter large motions and rates due to ocean disturbances. In addition, the water resistance is increased by added resistance which may cause speed reduction and energy loss (Prpic-Orsic and Faltinsen, 2012). A study suggests that the magnitude of the added resistance is in the range 10%-30% of the resistance in still water (Arribas, 2007). From a commercial standpoint, fuel efficiency and energy conservation are being driven by business requirements in the marine industry (Armstrong, 2013). In the area of ship motion control, Liu and Jin (2013) have done some work on the relationship of rolling and added resistance and have also provided a practical PID method to design an optimal added resistance fin control system. Subsequently, Liu et al. (2014) proposed a double Nonlinear Generalised Minimum Variance (NGMV) anti-roll control system to try to reduce the speed reduction. Yaw motion due to steering can also lead to added resistance in calm water as well as in waves. Grimble and Katebi (1986) extended a Linear Quadratic Gaussian (LQG) controller to minimise energy reduction and added resistance induced by steering in ship course keeping control. Miloh and Pachter (1989) also considered this kind of speed loss in a ship collision avoidance control system. Kim et al. (2015) studied the variation of ship's speed under different rudder controllers and results show that a ship's speed in regular waves may be improved by decreasing the rudder rotation velocity. Liu et al. (2016) combined both the added resistance in waves and calm water and suggested a Rudder Roll Stabilisation (RRS) control system with forward speed loss minimisation. In all these studies, the design of the control system was made under the condition of the ship moving with a certain constant speed and ship dynamics were not changed by the speed. In reality, the changes in the ship model parameters when sailing in open seas are mostly due to changes in the ship speed. The forward speed is time-varying because of the speed loss which may lead to the vessel dynamics and control parameters changing. The purpose of this paper is to design a ship autopilot control system with forward speed maintenance, considering unknown stochastic wave disturbances and parameter uncertainties caused by ship speed reduction.

The rest of this paper is organised as follows. Section 2 describes the ship dynamics and the added resistance. Section 3 presents the system structure and controller design. Simulation results and the performance of the proposed control system are discussed in Section 4. Conclusions are drawn in Section 5.

2. PROBLEM FORMULATION.

The study of ship motion is very complex because a set of parameters need to be determined in the motion dynamics. In this section, the mathematical models for the ship dynamics are presented using a modification of the experimental results developed by Perez (2005).

2.1. *Sway-yaw dynamics.*

The mathematical model for ship dynamics is introduced for a naval vessel. The dynamic equations of motion and corresponding forces in the body

https://doi.org/10.1017/S0373463318001078 Published online by Cambridge University Press

fixed frame can be represented as:

$$(m - Y_{\dot{v}})\dot{v} + (mx_G - Y_{\dot{r}})\dot{r} = Y_{|U|v}\,|U|\,v + Y_{Ur}Ur + Y_{v|v|}v\,|v| + Y_{v|r|}v\,|r| + Y_{r|v|}r\,|v| - mUr + Y_c \quad (1)$$

$$(mx_G - N_{\dot{v}})\dot{v} + (I_{zz} - N_{\dot{r}})\dot{r} = N_{|U|v}\,|U|\,v + N_{|U|r}\,|U|\,r + N_{r|r|}r\,|r| + N_{r|v|}r\,|v| - mx_GUr + N_c \quad (2)$$

$$\dot{\psi} = r \quad (3)$$

where m is the ship mass and I_{zz} is inertia. x_G are the coordinates of the centre of gravity with respect to the body fixed frame. Sway velocity is represented by v. Yaw and its angular velocity are denoted by ψ and r, respectively. Y and N are external forces with respect to sway and yaw. Subscript c denotes the force or moment produced by the control surface.

The rudder is the device used for heading control here. The rudder induced forces and moments can be expressed in the following:

$$Y_c = \frac{1}{2}\rho A_R C_L U^2 \quad (4)$$

$$N_c = -\frac{1}{2}\rho A_R C_L U^2 LCG \quad (5)$$

where ρ is the water density, A_R is the area of the rudder, C_L is the lift coefficient which varies with the effective angle of attack and LCG is the distance from the centre of gravity to the rudder stock.

2.2. *Steering model.* The ship steering system in this study is an underactuated system where the sway motion cannot be directly controlled. The study aims to achieve ship course keeping, so only yaw motion is considered. Combining the rudder action $N_c = N_\delta\delta$ and the wave disturbance, the steering dynamics can be treated as:

$$(I_{zz} - N_{\dot{r}})\dot{r} = N_{|U|r}\,|U|\,r + N_{r|r|}r\,|r| - mx_GUr + N_\delta\delta + d_w \quad (6)$$

where δ is rudder angle and d_w is the yaw moment caused by waves.

In practice, the dynamics of the ship and actuator are changed by the time varying speed which causes parameter uncertainties. The upper bounds of disturbance and parameter uncertainties are often difficult to find. The uncertainties in a system are assumed to meet the matching conditions. In this section, a modified control model is presented, considering the time varying speed $U(t) = U_0 + \Delta U$ due to the speed loss, where U_0 is the nominal (designed) speed and ΔU is the time varying speed loss which is unknown but bounded. The steering model is written as:

$$\dot{r} = a_1(U)r + a_2 r\,|r| + a_3\delta + a_4 d_w \quad (7)$$

where $a_1(U) = \frac{N_{|U|r}|U| - mx_GUr}{I_{zz} - N_{\dot{r}}}$, $a_2 = \frac{N_{r|r|}}{I_{zz} - N_{\dot{r}}}$, $a_3 = \frac{N_\delta}{I_{zz} - N_{\dot{r}}}$, $a_4 = \frac{1}{I_{zz} - N_{\dot{r}}}$

Considering the dynamic uncertainties caused by the speed loss, the steering model is revised as:

$$\dot{r} = a_1(U_0)r + a_2 r\,|r| + a_3\delta + d \quad (8)$$

where $d = d_1 + d_2 = a_1(\Delta U)r + a_4 d_w$ is the lumped uncertainties, d_1 is the internal disturbance and d_2 is the external disturbance.

https://doi.org/10.1017/S0373463318001078 Published online by Cambridge University Press

Assumption 1: The position and rate measurements of the yaw motion of the vehicle are available for feedback. The gyroscopic compass measures ψ and the yaw rate gyro measures r.

Assumption 2: The disturbance signal satisfies $|d(t)| \leq d_{\max}$ and $d_{\max}$ is an unknown positive constant.

Remark 1: The sway motion cannot be directly controlled, but it is influenced by the yaw motion control commanded rudder angle.

2.3. *Wave model.* Complex sea states are considered to be the superposition of an infinite number of monochromatic waves, distributed in all directions. In order to simulate random waves, an International Towing Tank Conference (ITTC) long-crest wave spectrum is adopted to recreate a fully developed sea environment. The equation of wave Power Spectral Density (PSD) is given as follows:

$$S(\omega_i) = \frac{173 H_{1/3}}{T^4 \omega_i^5} \exp\left(-\frac{691}{T^4 \omega_i^4}\right) \tag{9}$$

where $H_{1/3}$ is the significant wave height, T is the wave period and ω_i is the wave frequency of the i-th regular wave component.

In this paper, 60 regular wave components are used to form an irregular wave. The amplitude of each regular wave component ζ_i and the resultant wave ζ can be obtained by the following equations:

$$\zeta_i = \sqrt{2S(\omega_i)\,\Delta\omega} \tag{10}$$

$$\zeta = \sum_{i=1}^{60} \zeta_i \cos(\omega_i t + \varepsilon_i) \tag{11}$$

where ε_i is the random phase angle of the $i-$th regular wave, which ranges from 0 to 2π. In this calculation, the resultant wave ζ is used to calculate the external forces. This calculation is performed using code prepared in MATLAB, along with the calculation of the wave excitation forces and moments.

Generally, when a vessel is sailing with a constant speed, the wave frequency is modified as the encounter frequency and it is expressed as follows:

$$\omega_{ei} = \omega_i - \frac{\omega_i^2}{g} \cos\beta \tag{12}$$

where β is the encounter angle, g is the gravitational acceleration.

In order to simulate the time series of external disturbances accurately, the time domain model of the yaw moment caused by waves is derived with the strip theory

https://doi.org/10.1017/S0373463318001078 Published online by Cambridge University Press

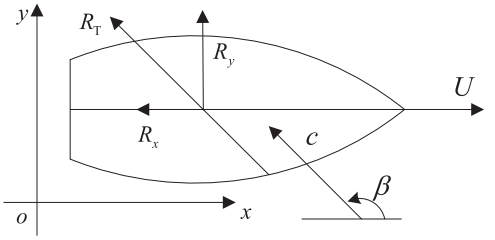

Figure 1. Definition of added resistance and drift force.

(Bhattacharyya, 1978) and it is given as follows:

$$d_w = \sum_{i=1}^{n} [d_{i1}\zeta_i \cos(\omega_{ei}t + \varepsilon_i) + d_{i2}\zeta_i \sin(\omega_{ei}t + \varepsilon_i)] \tag{13}$$

where $d_{i1} = 2\rho g \sum_{j=1}^{N} \{\exp(-k_i T_j/2) T_j x_j \sin[k_i B_j \sin(\beta/2)] \cos(k_i x_j \cos\beta)\Delta x\}$, ρ is the water density, and $d_{i2} = 2\rho g \sum_{j=1}^{N} \{\exp(-k_i T_j/2) T_j x_i \sin[k_i B_j \sin(\beta/2)] \sin(k_i x_i \cos\beta)\Delta x\}$. ζ_i and k_i are the wave amplitude and the wave number of the wave component i. N and Δx are the section number of the ship and the length of each section. T_j, B_j and x_j are draft, breadth and the coordinate point of the section j, respectively.

2.4. *Added resistance.* Generally, the design of propulsive power of a ship is based on still water resistance, which will be a constant when sailing on the open sea. The forward speed will be reduced due to the added resistance which is independent of the calm water resistance. In the following we consider the added resistance caused by ship motions both in waves and in still water.

In oblique waves, the force and moment which should be applied externally can be separated according to energy considerations. The force along the x-axis (added resistance) expends energy, whereas the one along the y-axis (drift force) does not expend energy. These forces are calculated by the method proposed by Loukakis and Sclavounos (1978). As shown in Figure 1, the ship is moving forward along a fixed direction. The waves arrive at an encounter angle β with a speed of propagation c. The horizontal force R_T can be resolved into two components, the added resistance R_x and the drift force R_y.

According to the extended radiated energy theory (Loukakis and Sclavounos, 1978), the work of the added resistance is assumed to equate to the energy contained in the dumping waves radiated away from the ship during each wave period. The work of the horizontal force to the energy per encounter period radiated away from from the ship which moves with five degrees of freedom can be equated with strip theory approximations. Therefore, the work transformed to the fluid can therefore be expressed as:

$$P = (-R_T)(-c - U\cos\beta)T_e \tag{14}$$

where T_e is the encounter period.

Since the purpose of this study is the control of underactuated vessels, the general Six Degree of Freedom (6-DOF) motions can be reduced to the motion in sway and yaw (that

https://doi.org/10.1017/S0373463318001078 Published online by Cambridge University Press

is, horizontal motions) under the assumption that the only available control input is rudder angle. For the energy radiated from the ship sideways, we obtain the energy radiated by the horizontal motions:

$$P_{26} = \frac{\pi}{\omega_e} \int_L b_{26} |U_{RY}|^2 \, \mathrm{d}x \tag{15}$$

where ω_e is the encounter frequency, L is the ship length and b_{26} is the motion damping coefficient. U_{RY} is the transverse relative velocity of each ship section. Hence, the formulae to calculate the added resistance and drift force in oblique waves are:

$$(-R_T)(-c - U\cos\beta)T_e = P_{26} \tag{16}$$

$$|R_x| = |R_T \cos\beta| \tag{17}$$

$$\left|R_y\right| = |R_T \sin\beta| \tag{18}$$

where P_{26} is the energy radiated by sway-yaw motion during one encounter period.

In the calm water case, when the ship travels with a yaw angle, it will create a pressure difference between the port and starboard of the ship and lead to an extra resistance, which gives a contribution to the longitudinal response of the ship. The longitudinal component of Newton's second law in the body fixed coordinate system is:

$$M(\dot{u} - vr) = X_{\dot{u}}\dot{u} - R_T(u) + (1 - \tau)T(u, n) + X_{vv}v^2 + X_{vr}vr + X_{rr}r^2 + X_{\delta\delta}\delta^2 \tag{19}$$

where $X_{\dot{u}}, X_{vv}, \ldots$ are used to express longitudinal hydrodynamic forces on the hull and the rudder. $R_T(u)$ is the ship calm resistance, τ is the thrust deduction coefficient, $T(u, n)$ is the propeller revolutions per second and δ denotes the rudder angle.

The main cause of resistance increase in a turning motion is due to the terms Mvr and $X_{vr}vr$. Both $R_T(u)$ and $T(u, n)$ are independent of the steering motion. The terms X_{vv} and X_{rr} are defined to be zero if the ship is symmetrical according to potential flow theory. The term $X_{\delta\delta}\delta^2$ is the extra drag due to rudder angle and can be neglected because of its small value.

So, the added resistance due to yawing can be simplified to the following:

$$R_{yaw} = (M + X_{vr})vr \tag{20}$$

where M is the ship mass and this resistance will be decided by the value of sway rate and yaw angle velocity.

Assumption 3: The measurement of sway can be obtained either by using a compact 6-DOF sensor or Fibre Optic Gyroscopes (FOGs) to provide continuous and accurate measurement of 6-DOF motions (MARIN, 2014).

3. CONTROL SYSTEM. The proposed closed loop autopilot system is proposed in Figure 2. Here, ψ_d is the predetermined heading angle and the other desired values are set to zero. d_w represents the ocean environment disturbance and the structure of the steering machine is presented in Figure 3 which presents the relationship between the commanded rudder angle and the presented rudder angle. This block diagram is a simplified hydraulic machinery model and the characteristics of this model are important since they can induce

https://doi.org/10.1017/S0373463318001078 Published online by Cambridge University Press

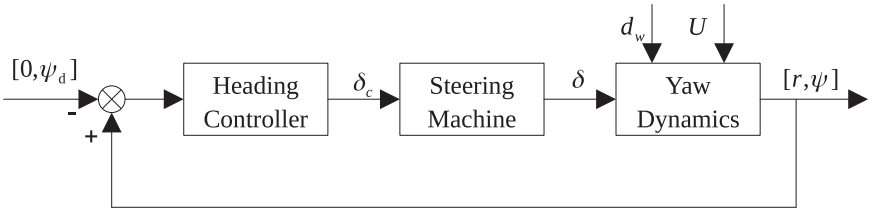

Figure 2. Autopilot control system.

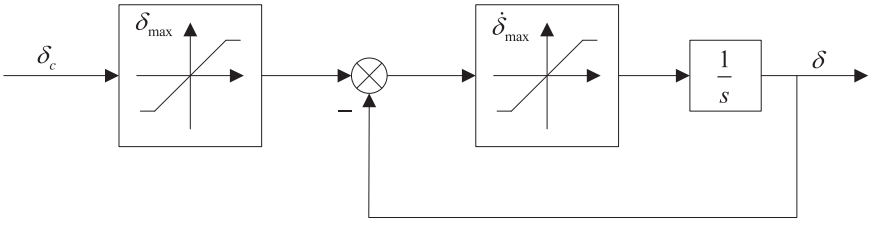

Figure 3. Steering machine model.

constraints on the control action, including magnitude saturation (that is, the rudder angle is constrained by the maximum angle δ_{max}) and rate saturation (that is, the rudder rate is limited by a maximum value $\dot{\delta}_{max}$).

The sliding mode control used here is a particular type of variable structure control that can accommodate system uncertainties and it can also reject external bounded disturbances as well as quantifying the modelling and performance trade-off. Liu et al. (2016) adopted the SMC method to design a RRS control system with forward speed minimisation which assumed U in the ship model was a constant design speed. However, the actual forward speed varies with the speed loss in the time domain which can cause uncertainties in the dynamics of ship and actuator, which then decreases the robustness of the SMC. To improve the performance of the controller when the speed is varying over time, the following sections present the design process of two controllers.

3.1. *Adaptive sliding mode controller.* Considering Equation (8), the nonlinear steering system contains a nonlinear term; the feedback linearization method is adopted to convert the nonlinear part. By defining a new control signal u, the rudder angle order can be treated as follows:

$$\delta_c = \frac{1}{a_3}(u - a_2 r|r|) \tag{21}$$

Then the nonlinear steering system is expressed in a linear equation:

$$\dot{r} = a_1(U_0)r + u + d \tag{22}$$

The state space format is:

$$\dot{\mathbf{x}} = \mathbf{A}\mathbf{x} + \mathbf{B}u + d \tag{23}$$

where $\mathbf{x} = \begin{bmatrix} r \\ \psi \end{bmatrix}$, $\mathbf{A} = \begin{bmatrix} a_1 & 0 \\ 1 & 0 \end{bmatrix}$, $\mathbf{B} = \begin{bmatrix} 1 \\ 0 \end{bmatrix}$.

https://doi.org/10.1017/S0373463318001078 Published online by Cambridge University Press

Let the reference state be $\mathbf{x}_d = [0, \psi_d]$ and $\dot{\mathbf{x}}_d = 0$. A sliding manifold is used to obtain the control law and is defined as:

$$s = \mathbf{h}^T \mathbf{x}_e = \mathbf{h}^T (\mathbf{x} - \mathbf{x}_d) \tag{24}$$

where $\mathbf{h} = [h_1, h_2]^T$ is a right eigenvector of $\mathbf{A}_c$ (i.e. $\mathbf{A}_c^T \mathbf{h} = \lambda \mathbf{h}$). The weighting vector $\mathbf{h}$ is selected by computing the equation $\mathbf{A}_c^T \mathbf{h} = 0$ for $\lambda = 0$ (Healey and Lienard, 1993).

In the SMC system, a feedback control law is written as:

$$u = -\mathbf{k}\mathbf{x} + u_0 \tag{25}$$

where the first item of the controller is a state feedback control law (that is, an equivalent controller), the second term is a nonlinear switching control law.

Substituting Equation (25) into Equation (23), we obtain:

$$\dot{\mathbf{x}} = \mathbf{A}_c \mathbf{x} + \mathbf{B} u_0 + d \tag{26}$$

where $\mathbf{A}_c = \mathbf{A} - \mathbf{B}\mathbf{k}^T$ is the combined state matrix, $\mathbf{k} = [k, 0]^T$ is the feedback gain vector and the zero gain in $\mathbf{k}$ represents the integration in the yaw angle channel.

The nonlinear switching control law to reject the disturbance is chosen as follows:

$$u_0 = -(\mathbf{h}^T \mathbf{B})^{-1} [\mathbf{h}^T \hat{d} + \eta \mathrm{sgn}(s)] \tag{27}$$

where $\hat{d}$ is the estimate of d.

Differentiating the sliding surface function, then:

$$\dot{s} = \mathbf{h}^T \mathbf{A}_c \mathbf{x} + \mathbf{h}^T \mathbf{B} u_0 + \mathbf{h}^T d - \mathbf{h}^T \dot{\mathbf{x}}_d = \lambda \mathbf{x}^T \mathbf{h} - \eta \mathrm{sgn}(s) + \mathbf{h}^T \Delta d = -\eta \mathrm{sgn}(s) + \mathbf{h}^T \Delta d \tag{28}$$

where $\lambda \mathbf{x}^T \mathbf{h} = 0$ if $\mathbf{h}$ is a right eigenvector, and $\mathbf{h}^T \dot{\mathbf{x}}_d = 0$ because the reference signal $\mathbf{x}_d$ is a constant vector. The parameter $\Delta d = d - \hat{d}$ is the estimation error.

Since the disturbance is unknown, a better guess for it is $\hat{d} = 0$. Hence, the nonlinear switching control law becomes:

$$u_0 = -(\mathbf{h}^T \mathbf{B})^{-1} \eta \mathrm{sgn}(s) \tag{29}$$

where $\eta > d_{\max} \|\mathbf{h}\|$.

Equation (29) leads to the sliding mode controller:

$$\delta_c = \frac{1}{a_3} \left[-kr - \frac{1}{h_1} \eta \mathrm{sgn}(s/\varphi) - a_2 r |r| \right] \tag{30}$$

In this controller, a larger switching gain η corresponds to a shorter time to reach $s = 0$ and the system robustness against the environmental disturbance is proven. However, the upper bound of disturbance is often difficult to find in practice. So, the adaptive method is adopted to tune the controller gain without knowledge about the disturbance. Still considering the estimate of the disturbance is zero, the robust switching control law of the total controller is modified as:

$$u_0 = -(\mathbf{h}^T \mathbf{B})^{-1} \hat{\eta} \mathrm{sgn}(s) \tag{31}$$

where $\hat{\eta}$ is the estimate of the adjustable gain and is a positive value.

https://doi.org/10.1017/S0373463318001078 Published online by Cambridge University Press

The adaptation law is written as:

$$\dot{\hat{\eta}} = \frac{1}{\alpha}|s| \tag{32}$$

where $\alpha > 0$ is the adaptation gain.

Then the differentiation of the sliding surface is:

$$\dot{s} = \mathbf{h}^{\mathrm{T}}(\dot{\mathbf{x}}\text{-}\dot{\mathbf{x}}_{\mathrm{d}}) = \mathbf{h}^{\mathrm{T}}(\mathbf{A}_{\mathrm{c}}\mathbf{x} + \mathbf{B}u_0 + d) = \mathbf{h}^{\mathrm{T}}\mathbf{B}u_0 + \mathbf{h}^{\mathrm{T}}d = -\hat{\eta}\mathrm{sgn}(s) + \mathbf{h}^{\mathrm{T}}d \tag{33}$$

Selecting the Lyapunov function,

$$V = \frac{1}{2}s^2 + \frac{1}{2}\alpha\tilde{\eta}^2 \tag{34}$$

where $\tilde{\eta} = \hat{\eta} - \eta$ is the estimation error.

$$\begin{aligned}\dot{V} &= \frac{1}{2}s\dot{s} + \frac{1}{2}\alpha\tilde{\eta}^2 = s[\mathbf{h}^{\mathrm{T}}d - \hat{\eta}\mathrm{sgn}(s)] + \alpha(\hat{\eta} - \eta)\dot{\hat{\eta}} \\ &= s\mathbf{h}^{\mathrm{T}}d - \hat{\eta}|s| + (\hat{\eta} - \eta)|s| = s\mathbf{h}^{\mathrm{T}}d - \eta|s| \le 0\end{aligned} \tag{35}$$

Equation (35) holds for all time for the external disturbance. The parameter $\hat{\eta}$ chosen in Equation (31) implies that the system trajectory will move and reach the sliding surface in a finite time and the sliding surface declines to zero, so the control law given by Equation (25) guarantees the sliding mode sustained (Huang et al., 2013). The *tanh* function has replaced the *signum* function to attenuate the chattering effect. Hence, the Adaptive Sliding Mode Controller (A-SMC) is:

$$\delta_c = \frac{1}{a_3}[-kr - \frac{1}{h_1}\hat{\eta}\tanh(s/\varphi) - a_2 r|r|] \tag{36}$$

where φ is the boundary layer thickness.

3.2. *Nonlinear disturbance observer.* In the last section, the estimate of disturbance is treated as zero because no knowledge of the disturbance can be available. An alternative method to process this problem is called a Disturbance Observer (DO). Since the yaw acceleration is not easy to obtain, it is also difficult to construct the acceleration signal from yaw rate by differentiation. So, a modified observer called a Nonlinear Disturbance Observer (NDO) is adopted here (Chen, 2004; Yang et al., 2013).

Define a variable:

$$z = \hat{d} - p(r, \psi) \tag{37}$$

Let the function $p(r, \psi)$ be given by the following equation:

$$\frac{\mathrm{d}p}{\mathrm{d}t} = \frac{L(r, \psi)}{a_4}\dot{r} \tag{38}$$

Define the observer error signal:

$$\tilde{d} = d - \hat{d} \tag{39}$$

https://doi.org/10.1017/S0373463318001078 Published online by Cambridge University Press

According to the linear disturbance observer, a DO is proposed as:

$$\begin{aligned}\dot{\hat{d}} &= L(r,\psi)(d-\hat{d}) = L(r,\psi)(\dot{r} - a_1(U_0)r - a_2 r|r| - a_3\delta) - L(r,\psi)\hat{d} \\ &= L(r,\psi)(\dot{r} - a_1(U_0)r - a_2 r|r| - a_3\delta) - L(r,\psi)[z + p(r,\psi)] \\ &= -L(r,\psi)z + L(r,\psi)[\dot{r} - a_1(U_0)r - a_2 r|r| - a_3\delta - p(r,\psi)]\end{aligned} \tag{40}$$

In general, prior information about the derivative of the disturbance is unavailable, and the disturbance varies slowly relative to the observer dynamics. Then it reasonable to suppose that:

$$\dot{d} = 0 \tag{41}$$

Hence, the derivative of the observer error is:

$$\dot{\tilde{d}} = \dot{d} - \dot{\hat{d}} = -\dot{\hat{d}} = -L(r,\psi)\tilde{d} \tag{42}$$

Let the functions in Equation (36) be chosen as:

$$L(r,\psi) = a \tag{43}$$

where a is a positive constant.

Then the following equations are obtained:

$$p(r,\psi) = ar \tag{44}$$

$$\frac{\mathrm{d}p}{\mathrm{d}t} = a\dot{r} \tag{45}$$

Combining the above equations, the update law can be written as:

$$\begin{aligned}\dot{z} &= \dot{\hat{d}} - \frac{\mathrm{d}p}{\mathrm{d}t} = \dot{\hat{d}} - L(r,\psi)\dot{r} \\ &= -L(r,\psi)z + L(r,\psi)[-a_1(U_0)r - a_2 r|r| - a_3\delta - p(r,\psi)] \\ &= -az + a\{-[a + a_1(U_0)]r - a_2 r|r| - a_3\delta\}\end{aligned} \tag{46}$$

Hence, the NDO is given by:

$$\hat{d} = z + ar \tag{47}$$

The nonlinear switching control law in this SMC is defined as:

$$u_0 = -(\mathbf{h}^{\mathrm{T}}\mathbf{B})^{-1}[\mathbf{h}^{\mathrm{T}}\hat{d} + \eta_0\,\mathrm{sgn}(s)] \tag{48}$$

The differentiation of the sliding surface is:

$$\dot{s} = \mathbf{h}^{\mathrm{T}}\mathbf{A}_{\mathrm{c}}\mathbf{x} - \eta_0\,\mathrm{sgn}(s) + \mathbf{h}^{\mathrm{T}}d - \mathbf{h}^{\mathrm{T}}\hat{d} = \mathbf{h}^{\mathrm{T}}\mathbf{A}_{\mathrm{c}}\mathbf{x} - \eta_0\,\mathrm{sgn}(s) + \mathbf{h}^{\mathrm{T}}\tilde{d} = -\eta_0\,\mathrm{sgn}(s) + \mathbf{h}^{\mathrm{T}}\tilde{d} \tag{49}$$

Let the Lyapunov function be chosen as:

$$V = \frac{1}{2}s^2 + \frac{1}{2a}\tilde{d}^2 \tag{50}$$

https://doi.org/10.1017/S0373463318001078 Published online by Cambridge University Press

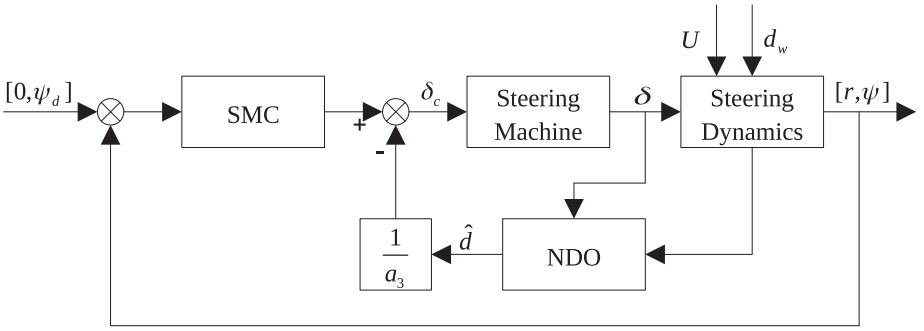

Figure 4. Modified autopilot control system.

Differentiation of the Lyapunov function with respect to the trajectory of states gives:

$$\dot{V} = s\dot{s} + \frac{1}{a}\tilde{d}\dot{\tilde{d}} = -\eta_0 \operatorname{sgn}(s) + \mathbf{h}^{\mathrm{T}}\tilde{d}s - a\tilde{d}^2 \leq 0 \tag{51}$$

where the gain must satisfy $\eta_0 > \|\mathbf{h}\| \cdot \left\|\tilde{d}\right\|$.

Hence, the final output of the sliding mode controller with nonlinear disturbance observer (NDO-SMC) is written as:

$$\begin{aligned}\delta_c &= \frac{1}{a_3}[-kr - \hat{d} - \frac{1}{h_1}\eta_0 \tanh(s/\varphi) - a_2 r|r|] \\ &= \frac{1}{a_3}[-kr - \frac{1}{h_1}\eta_0 \tanh(s/\varphi) - a_2 r|r|] - \frac{1}{a_3}\hat{d}\end{aligned} \tag{52}$$

where the first term in Equation (52) can be treated as a sliding mode controller that rejects the disturbance $\tilde{d}$. A diagram of this control system is shown in Figure 4.

4. SIMULATION RESULTS. A heading control system simulation of a naval vessel is demonstrated (Perez, 2005). The nominal ship speed is 15 knots and it is assumed to be sailing in a sea environment that is infinitely deep. The wave disturbance is simulated with a significant wave height of 2 m and an average period of 7·5 s. In order to avoid the effect of stall angle the magnitude constraint for the rudder angle of $\delta_{\max} = \delta_{stall} = 25^\circ$ and the vessel is equipped with two rudders. The maximum rudder rate is $\dot{\delta}_{\max} = 15^\circ/s$. The desired state trajectory is assumed to be $\mathbf{x}_{\mathrm{d}} = (0,0)^{\mathrm{T}}$, the initial state vector is $\mathbf{x} = (0,0)^{\mathrm{T}}$, the initial guess of η is 2 for the SMC. The initial values of the adaptation law are set as $\eta(0) = 2$ and $\eta_0(0) = 1{\cdot}5$. The boundary layer is chosen as $\varphi = 1$. The linear state feedback gain is $k = 0{\cdot}1$ and $(\eta_{\min}, \eta_{\max})$ is considered as $(1, 10)$. The nonlinear disturbance observer parameter is selected as $a = 20$. The vessel sails in an oblique wave condition with an encounter angle of 135° and the time domain simulation is done by a fourth order Runge-Kutta (Fossen, 2011) numerical integration method with the time step of 0·1 s.

The computation simulations of a course keeping manoeuvre of a nonlinear ship autopilot system are presented in Figures 5 to 10, and the corresponding simulation values (Root Mean Square (RMS) value) are presented in Table 1. Figure 5 shows the time series of wave

https://doi.org/10.1017/S0373463318001078 Published online by Cambridge University Press

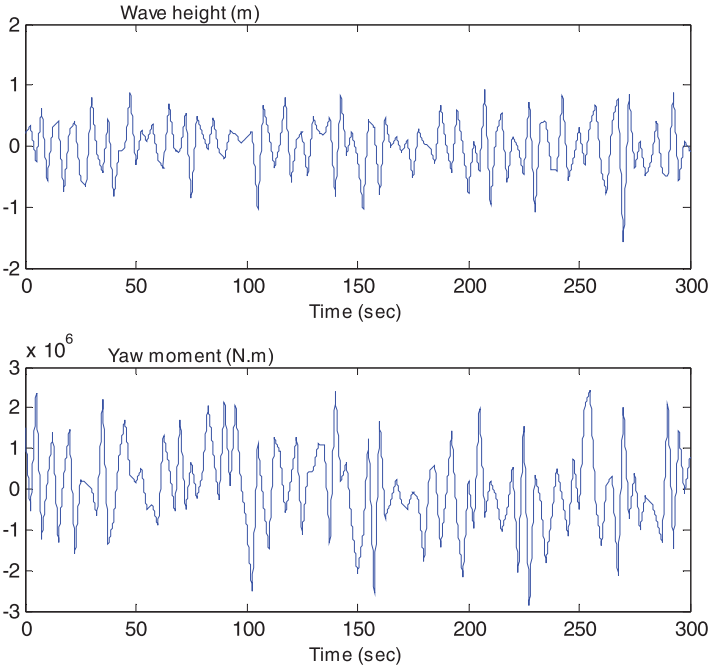

Figure 5. Time series of wave height and yaw moment.

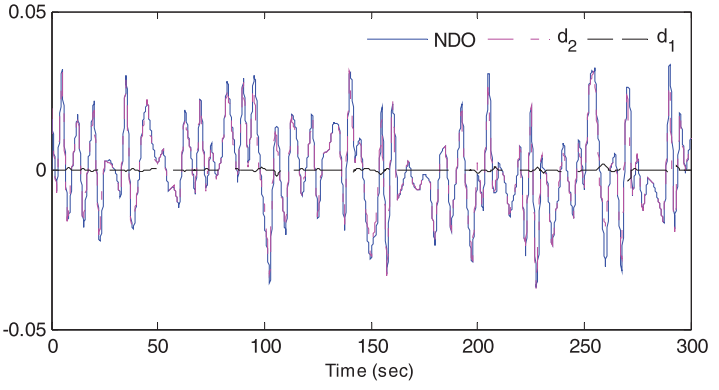

Figure 6. Simulation results of the disturbance observer.

height sand yaw moments which represent the external disturbance. Figure 6 presents non-dimensional results of the proposed observer, where d_1 is the internal disturbance (that is, the system uncertainties caused by the speed loss) and d_2 is the external disturbance (the yaw moment caused by waves). A better NDO performance can be obtained when a larger value of $L(r, \psi)$ is chosen, since an overlarge value can cause an algebraic loop problem in the process of numerical calculation, the value ($a = 20$) used in this study is reasonable.

Figure 7 shows the simulation of sway rate and yaw rate which could induce added resistance in both waves and calm water according to Equations (13) and (18). The dashed

https://doi.org/10.1017/S0373463318001078 Published online by Cambridge University Press

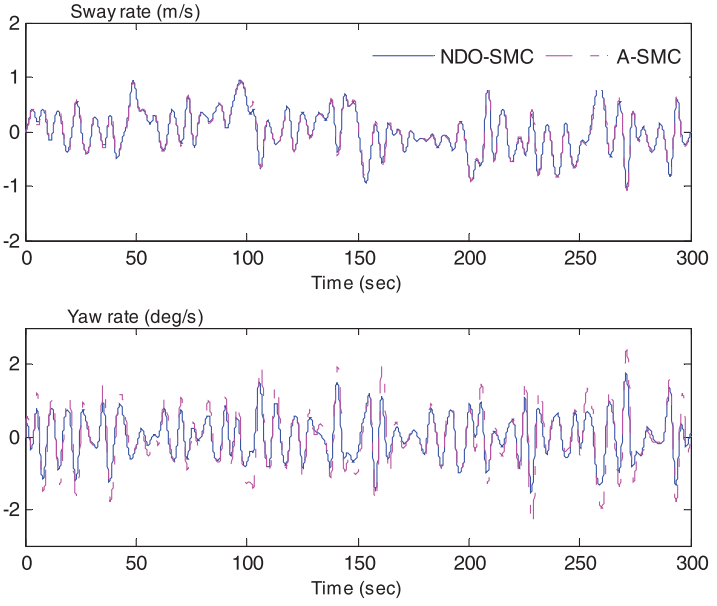

Figure 7. The comparison of sway rate and yaw rate.

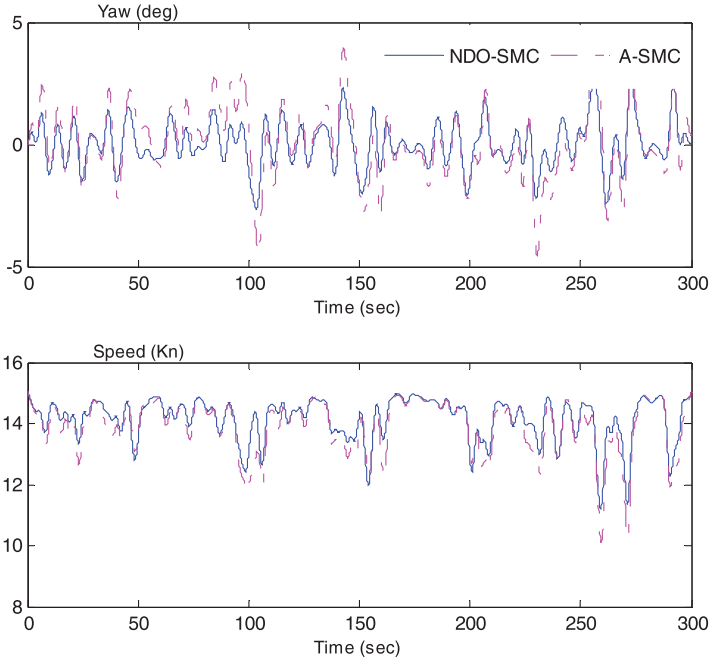

Figure 8. The comparison of yaw angle and speed.

https://doi.org/10.1017/S0373463318001078 Published online by Cambridge University Press

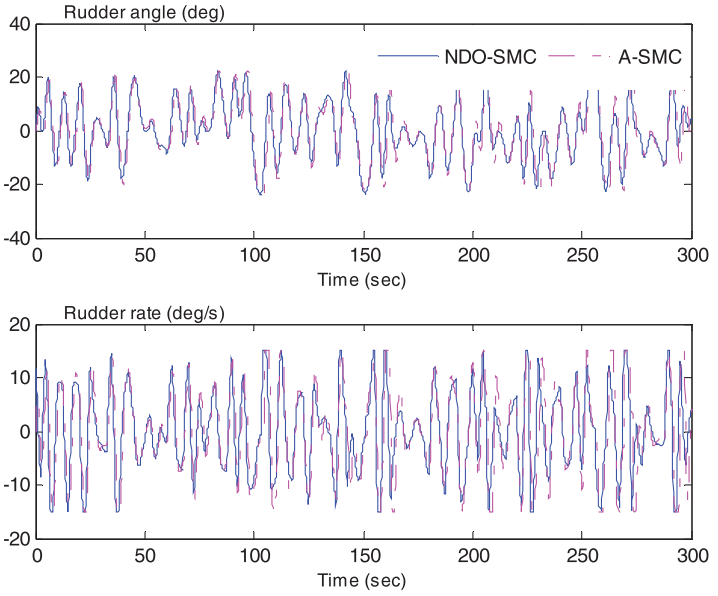

Figure 9. The comparison of rudder angle and rate.

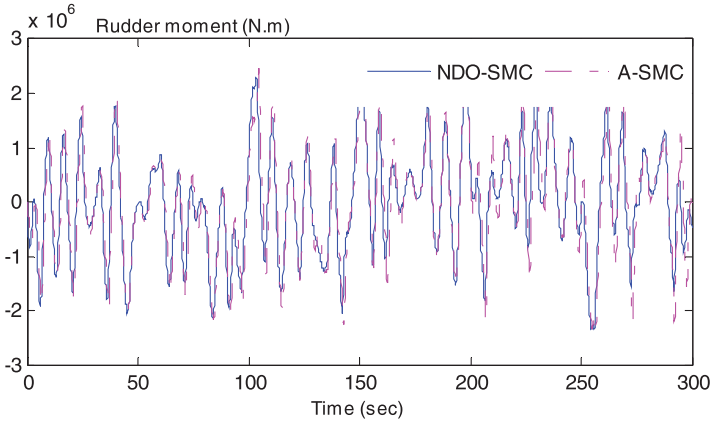

Figure 10. The comparison of rudder moment.

Table 1. Cost values of simulation.

Performance (RMS)	NDO-SMC	A-SMC	Unit
Sway rate	0·38	0·39	m/s
Yaw angle	0·93	1·47	deg
Yaw rate	0·59	0·82	deg/s
Rudde rangle	10·72	11·47	deg
Rudder rate	7·49	8·32	deg/s
Average speed	14·14	13·89	kn

https://doi.org/10.1017/S0373463318001078 Published online by Cambridge University Press

lines represent the time series of the adaptive sliding mode controller while the solid lines mean the time response of the sliding mode controller with NDO. The NDO-SMC can achieve smaller values of sway velocity and yaw rate, see Table 1 (0·38 and 0·59, respectively). That is to say, the added resistance due to sway–yaw coupling motion in waves and the added resistance by yawing motion in calm water have declined, compared with the A-SMC method. Hence, the NDO-SMC method can maintain the forward speed more effectively, as shown in Figure 8, and the mean value of the forward speed can be raised by 0·25 knots as against the A-SMC method which cannot be ignored in a real voyage of a vessel. Figure 8 also presents the heading control performance; the yaw response is significantly improved by the proposed NDO-SMC algorithm.

Figure 9 presents a comparison of rudder commands. The A-SMC method causes larger amplitudes of rudder angle and rudder rate; the additional rudder command may cost more energy to drive actuators and cause rudder angle and rate saturation, which may enhance the mechanical wear and tear of actuators. This is also the reason why a saturation element is needed. The values calculated from the cost function are listed in Table 1. Thus, the A-SMC scheme can produce a greater rudder moment to reject the wave moment because of the larger rudder angle, as shown in Figure 10, but it does not achieve a better sailing performance. The reason maybe that the NDO can estimate the disturbance more accurately and then the controller can give more suitable rudder commands to match the yaw moment.

5. CONCLUSION. Considering forward speed keeping, this paper has discussed two sliding mode controllers to deal with the total unknown bounded disturbance for a nonlinear vessel steering control system, based on an adaptive controller and the nonlinear disturbance observer method. As presented in the simulation results, all controllers have successfully converged the ship actual course into the reference course and maintained the ship speed effectively, especially the proposed NDO-SMC scheme. As noted in the simulations, the rudder response can approach the limitation of rudder angle and rudder rate due to the control output signals requirement. The vessel autopilot system performance is evaluated under a trade-off between the rudder control gain and a faster course keeping response. Comparing the control performance, the ship heading response under the nonlinear observer method represents the superior performance that requires lower rudder actuations and better heading response.

REFERENCES

Alfardo-Cid, E., McGookin, E.W., Murray-Smith, D.J. and Fossen, T.I. (2005). Genetic algorithms optimization of decoupled sliding mode controllers: simulated and real results. *Control Engineering Practice*, **13**(6), 739–748.

Arribas, F.P. (2007). Some methods to obtain the added resistance of a ship advancing in waves. *Ocean Engineering*, **34**(7), 946–955.

Armstrong, V.N. (2013). Vessel optimisation for low carbon shipping. *Ocean Engineering*, **73**, 195–207.

Banazadeh, A. and Ghorbani, M.T. (2013). Frequency domain identification of Nomoto model to facilitate Kalman filter estimation and PID heading control of a patrol vessel. *Ocean Engineering*, **72**, 344–355.

Bhattacharyya, R. (1978). *Dynamics of marine vehicles*. John Wiley & Sons, New York.

Borkowski, P. (2014). Ship course stabilization by feedback linearization with adaptive object model. *Polish Maritime Research*, **21**(81), 14–19.

Burns, R.S. (1995). The use of artificial neural networks for the intelligent optimal control of surface ships. *IEEE Journal of Oceanic Engineering*, **20**(1), 65–72.

Chen, W.H. (2004). Disturbance observer-based control for nonlinear systems. *IEEE Transactions on Mechatronics*, **9**(4), 706–710.

Do, K.D. and Pan, J. (2006). Global robust adaptive path following of underactuated ships. *Automatica*, **42**(10), 1713–1722.

Do, K.D. (2015). Robust adaptive tracking control of underactuated ODINs under stochastic sea loads. *Robotics and Autonomous System*, **72**, 152–163.

Du, J., Hu, X., Krstic., M. and Sun, Y. (2016). Robust dynamic positioning of ships with disturbances under input saturation. *Automatica*, **73**, 207–214.

Fang, M.C. and Luo, J.H. (2005). The nonlinear hydrodynamic model for simulating a ship steering in waves with autopilot system. *Ocean Engineering*, **32**(11), 1486–1502.

Fang, M.C. and Luo, J.H. (2006). A combined control system with roll reduction and track keeping for the ship moving in waves. *Journal of Ship Research*, **50**(4), 344–354.

Fang, M.C. and Luo, J.H. (2007). On the tracking and roll reduction of the ship in random waves using different sliding mode controllers. *Ocean Engineering*, **34**(3), 479–488.

Fang, M.C., Lin, Y.H., and Wang, B.J. (2012). Applying the PD controller on the roll reduction and track keeping for the ship advancing in waves. *Ocean Engineering*, **54**(4), 13–25.

Fossen, T.I. (2011). *Handbook of Marine Craft Hydrodynamics and Motion Control*. Wiley Press, West Sussex.

Grimble, M.J. and Katebi, M.R. (1986). LQG design of ship steering control systems. *Signal Processing for Control, Lecture Notes in Control and Information Sciences*, **79**, 387–413.

Harl, N. and Balakrishnan, S.N. (2012). Impact time angle guidance with sliding mode control. *IEEE Transactions on Control System Technology*, **20**(6), 1436–1449.

Healey, A.J. and Lienard, D. (1993). Multivariable sliding mode control for autonomous diving and steering of unmanned underwater vehicles. *IEEE Journal of Oceanic Engineering*. **18**(3), 327–339.

Huang, Y.J., Kuo, T.C. and Chang, S.H. (2013). Adaptive sliding mode control for nonlinear systems with uncertain parameters. *IEEE Transactions on Systems, Man and Cybernetics. B Cybernetics*, **38**(2), 534–539.

Kim, S.S., Kim, S.D., Kang, D., Lee, J., Lee, S.J. and Jung, K.H. (2015). Study on variation in ship's forward speed under regular waves depending on rudder controller. *International Journal of Naval Architecture and Ocean Engineering*, **7**(2), 364–374.

Li, Z. and Sun, J. (2012). Disturbance compensating model predictive control with application to ship heading control. *IEEE Transactions on Control Systems Technology*, **20**(1), 257–265.

Lei, Z. and Guo, C. (2015). Disturbance rejection control solution for ship steering system with uncertain time delay. *Ocean Engineering*, **95**, 78–83.

Li, H., Liu, J., Hilton, C. and Liu, H. (2013). Adaptive sliding mode control for nonlinear active suspension vehicle systems using T-S fuzzy approach. *IEEE Transactions on Industrial Electronics*, **60**(8), 3328–3338.

Lin, C.M., Hsueh, C.S. and Chen, C.H. (2014). Robust adaptive backstepping control for a class of nonlinear systems using recurrent wavelet neural network. *Neurocomputing*, **142**, 372–382.

Liu, W., Sui, Q., Xiao, H. and Zhou., F. (2011). Sliding backstepping control for ship course with nonlinear disturbance observer. *Journal of Information and Computation Science*, **8**(14), 3809–3817.

Liu, Z. and Jin, H. (2013). Extended radiated energy method and its application to a ship roll stabilisation control system. *Ocean Engineering*, **72**(7), 25–30.

Liu, Z., Jin, H., Grimble, M.J. and Katebi, R. (2014). Ship roll stabilization control with low speed loss. *MTS/IEEE Oceans'14*, Taipei, Taiwan.

Liu, C., Sun, J. and Zou, Z. (2015). Integrated line of sight and model predictive control for path following and roll motion control using rudder. *Journal of Ship Research*, **59**(2), 99–112.

Liu, Y.C., Liu, S.Y. and Wang, N. (2016). Fully tuned fuzzy neural network robust adaptive tracking control of unmanned under water vehicle with thruster dynamics. *Neurocomputing*, **196**, 1–13.

Liu, Z., Jin, H., Grimble, M.J. and Katebi, R. (2016). Ship forward speed loss minimization using nonlinear course keeping and roll motion controllers. *Ocean Engineering*, **113**, 201–207.

Loukakis, T.A. and Sclavounos, P.D. (1978). Some extensions of the classical approach to strip theory of ship motions, including the calculation of mean added forces and moments. *Journal of Ship Research*, **22**, 1–19.

MARIN (2014). http://www.marin.nl/web/Research-Topics/Offshore-operations/Motion-monitoring.htm.

Miloh, T. and Pachter, M. (1989). Ship collision-avoidance and pursuit-evasion differential games with speed-loss in a turn. *Computers Mathematics with Application*, **18**(1), 77–100.

Moreira, L., Fossen, T.I. and Soares, C.G. (2007). Path following control system for a tanker ship model. *Ocean Engineering*, **34**(12), 2074–2085.

Peng, Z., Wang, D., Chen, Z., Hu, X. and Lan, W. (2013). Adaptive dynamic surface control for formations of autonomous surface vehicles with uncertain dynamics. *IEEE Transactions on Control System Technology*, **21**(2), 513–520.

Perez, T. (2005). *Ship Motion Control: Course Keeping and Roll Reduction Using Rudder and Fins*, Springer Press, London.

Perera, L. and Soares, C.G. (2012). Pre-filtered sliding mode control for nonlinear ship steering associated with disturbances. *Ocean Engineering*, **51**(3), 49–62.

Perera, L.P. and Soares, C.G. (2013). Lyapunov and Hurwitz based controls for input output linearization applied to nonlinear vessel steering. *Ocean Engineering*, **66**, 58–68.

Prpic-Orsic, J. and Faltinsen, O.M. (2012). Estimation of ship speed loss and associated CO2 emissions in a sea way. *Ocean Engineering*, **44**(1), 1–10.

Qin, z., Lin, Z., Sun, H. and Yang, D. (2016). Sliding mode control of path following for underactuated ships based on high gain observer. *Journal of Central South University*, **23**(10), 3356–3364.

Roberts, G.N. (2008). Trends in marine control systems. *Annual Review in Control*, **32**(2), 263–269.

Saari, H. and Djemai, M. (2012). Ship motion control using multi-controller structure. *Ocean Engineering*, **55**(4), 184–190.

Shojaei, K. (2015). Neural adaptive robust control of underactuated marine surface vehicles with input saturation. *Applied Ocean Research*, **53**, 267–278.

Tzeng, C.Y. (1999). An internal model control approach to the design of yaw rate control ship steering autopilot. *IEEE Journal of Oceanic Engineering*, **24**(4), 507–513.

Xu, D., Sun, Y., Du, J. and Hu, X. (2016). Disturbance observer based sliding mode controller design fir heave motion of surface effects ships. *Journal of Donghua University*, **33**(5), 759–763.

Yang, J., Li, S. and Yu, X. (2013). Sliding mode control for systems with mismatched uncertainties via a disturbance observer. *IEEE Transactions on Industrial Electronics*, **60**(1), 160–169.

Zhang, R., Chen, Y. and Sun, Z. (2000). Path control of a surface ship in restricted waters using sliding mode. *IEEE Transactions on Control System Technology*, **80**(4), 722–732.

Zhang, G., Zhang, X. and Zheng, Y. (2015). Adaptive neural path following control for underactuated ships in fields of marine practice. *Ocean Engineering*, **104**, 558–567.

Zhang, X. and Zhang, G. (2016). Design of a ship course keeping autopilot using a sine function based nonlinear feedback technique. *The Journal of Navigation*, **69**(2), 246–256.